Superparamagnetic relaxation in iron nanoclusters measured by low energy muon spin rotation



2000 J. Phys.: Condens. Matter 12 1399

(http://iopscience.iop.org/0953-8984/12/7/321)

J. Phys.: Condens. Matter **12** (2000) 1399–1411. Printed in the UK PII: S0953-8984(00)09872-6

# Superparamagnetic relaxation in iron nanoclusters measured by low energy muon spin rotation

T J Jackson†, C Binns‡, E M Forgan†, E Morenzoni§, Ch Niedermayer‖, H Glückler§, A Hofer‖§[+], H Luetkens§¶, T Prokscha§, T M Riseman†, A Schatz§¶, M Birke§¶, J Litterst¶, G Schatz‖ and H P Weber§

† Condensed Matter Group, School of Physics and Astronomy, University of Birmingham, Birmingham B15 2TT, UK
‡ Department of Physics and Astronomy, University of Leicester, Leicester LE1 7RH, UK
§ Paul Scherrer Institut, CH-5232 Villigen PSI, Switzerland
‖ Fakultät für Physik, Universität Konstanz, D-78434 Konstanz, Germany
¶ Institut für Metallphysik und nukleare Festkörperphysik, Technische Universität Braunschweig, D-38106 Braunschweig, Germany
[+] Tanner Documents, D-88131 Lindau, Germany

E-mail: t.j.jackson@bham.ac.uk

Received 25 November 1999

**Abstract.** Low energy (16 keV) muons were used to probe the dynamic magnetic behaviour of iron nanoclusters embedded in a silver thin film matrix. The silver film was 500 nm thick and contained a volume fraction of 0.1% iron. Measurements were made in a field of 25 mT, applied normal to the plane of the film, in the temperature range 4.7 K to 300 K. At temperatures above 20 K thermal activation of the cluster moments was seen as a narrowing of the field distribution sensed by the implanted muons. An intrinsic cluster relaxation time of $\tau_0 = 12 \pm 4$ ns and an activation energy of $51 \pm 9$ K were deduced from fits to the data. SQUID magnetometry of thicker (1.5 $\mu$m) but otherwise identical films on graphite substrates showed the clusters to have a volume of the order of $10^{-26}$ m$^3$, from which a cubic anisotropy constant of $K = 2.3 \pm 0.4 \times 10^5$ J m$^{-3}$ was calculated. Remanence measurements showed no evidence of a preferred orientation for the magnetization of the cluster assembly.

## 1. Introduction

The magnetization vector of a sufficiently small, single domain ferromagnetic particle may be observed to be unstable against thermal activation, a behaviour known as superparamagnetism [1]. The characteristic relaxation time of this process is an important parameter in contemporary magnetism, and has been extensively studied recently both experimentally [2–7] and theoretically [8–14]. The relaxation time provides a signature of the mechanism of magnetic reversal, allows the extraction of parameters such as anisotropy energies from experimental data and determines the long term stability of recording media based on fine magnetic particles.

Two widely used experimental techniques for studying superparamagnetic relaxation are Mössbauer spectroscopy and AC susceptibility measurements, which allow the relaxation to be probed over very different timescales. Recently, measurements of assemblies of iron nanoclusters yielded an intrinsic relaxation time of $\tau_0 = 1.0 \pm 0.5 \times 10^{-10}$ s and an anisotropy constant of $K = 1.2 \pm 0.2 \times 10^5$ J m$^{-3}$ [2]. Magnetization reversal in isolated cobalt particles

0953-8984/00/071399+13$30.00  

has also been observed, and a close agreement found with a theoretical analysis based upon thermal activation [3, 4].

Small angle elastic neutron scattering [5] provides a 'snapshot' of the magnetic order in thin film cluster samples. The neutrons pass through the sample over timescales far shorter than the relaxation times, providing a measure of the instantaneous magnetization. In addition, neutrons are sensitive to magnetic correlations between the clusters. More recently, inelastic neutron scattering and neutron spin echo spectroscopy have been used to observe superparamagnetism, in iron nanoparticles in an alumina thin film at a concentration of 20% iron [6]. Below 40 K interaction effects were significant but at higher temperatures relaxation appeared to be single-particle-like despite the high concentration. These authors discussed the importance of obtaining samples without a distribution of particle sizes for definitive studies of the dynamic magnetic behaviour.

Experiments have also been performed on bulk samples, prepared by metallurgical methods. For example, muon spin rotation ($\mu$SR) measurements of the relaxation of cobalt clusters embedded in a copper matrix showed intrinsic relaxation times at 35.4 K and 48.4 K of $1.4 \times 10^{-9}$ s and $3.7 \times 10^{-10}$ s respectively [7]. The relaxation rate was found to follow an Arrhenius law, i.e. $\tau^{-1} \propto \exp(-1/T)$. In general, the relaxation time is often written in an activated form

$$\tau = \tau_0 \exp(\Delta E / k_B T) \tag{1}$$

where in a domain of volume $V$, with cubic magnetocrystalline anisotropy $K$, the energy barrier $\Delta E$ is given by $\Delta E = KV/4$ [8].

In most theoretical treatments, the relaxation time is written in the form

$$\tau = \frac{2\tau_D}{\lambda_1} \tag{2}$$

where $\lambda_1$ represents the slowest relaxation mode, which dominates the relaxation time, and $\tau_D$, the diffusion relaxation time, is given by

$$\tau_D = \frac{V M_s (1 + a^2)}{2 k_B T \gamma_0 a}. \tag{3}$$

In equation (3), $M_s$ is the saturation magnetization and $\gamma_0$ is the gyromagnetic ratio, ($\gamma_0/2\pi = 31.7$ GHz T$^{-1}$ in bulk iron). The parameter $a$ is a dimensionless, phenomenological representation of the strength of dissipation processes which couple energy from the spin system to the lattice. For bulk iron, $a \approx 0.01$ but for small particles, or for particles which are highly defective, $a$ may be much larger, in the range $0.05 < a < 5$ [3, 4, 9].

Early considerations of cubic anisotropy [10] produced an expression for $\lambda_1$ in the limits $\Delta E / k_B T \geqslant 5$ and $a \Delta E / k_B T \geqslant 1$, and in zero applied field

$$\lambda_1 = \frac{8\sqrt{2}\alpha \exp(-\alpha/4) a}{\pi (1 + a^2)} \tag{4}$$

where the anisotropy parameter $\alpha = 4\Delta E / k_B T$. Equation (4) is included simply to show the connection between equations (1) and (2). More recent calculations valid over wide ranges of $\alpha$ and $a$ have been published [11], and recently progress towards calculations including the effects of an applied field has been reported [12]. In the limit $\Delta E / k_B T \leqslant 1$, $\lambda_1 = 2$, whatever the value of $a$ [11, 13]. In this limit, on inserting typical values for the cluster samples reported in this paper, relaxation times of the order of $10^{-9}$ s are predicted.

In this paper we present the first low energy muon spin rotation ($\mu$SR) measurements of superparamagnetic relaxation in a thin film cluster sample. In muon spin rotation, a beam of spin polarized muons is implanted in a sample. The muons occupy interstitial sites and

precess in the local magnetic field at a rate determined by the muon gyromagnetic ratio; $\gamma_\mu/2\pi = 135.5$ MHz T$^{-1}$. Muons are unstable, decaying with a lifetime of $\tau_\mu = 2.2$ $\mu$s into a positron and two neutrinos. The positron is emitted preferentially along the spin direction at the instant of decay, and so detection of the decay positrons yields a time spectrum from which the muon precession frequencies may be deduced. $\mu$SR methods are discussed in detail elsewhere [15, 16]. Thin film samples can not be investigated with conventional $\mu$SR spectrometers, because the kinetic energy of the incident muons is so high, at 4 MeV, that they would penetrate the film and become implanted in the substrate. A low energy $\mu$SR spectrometer has recently been developed at the Paul Scherrer Institut, specifically for studies of magnetism in thin films. The main muon beam is moderated in a van der Waals bound solid layer to energies of order 10 eV, and then accelerated to provide a beam of muons whose kinetic energy may be chosen from the range 0.5–30 keV [17, 18]. In metals, these energies correspond to implantation depths of order 5–300 nm [19]. The low energy $\mu$SR method allows the extension of the known advantages of $\mu$SR to very thin samples.

We used a thin film sample of iron clusters embedded in silver, with the clusters prepared in a gas condensation source [20]. Ionization of the iron cluster beam, followed by filtering in a mass spectrometer, allows a resolution of the order of two atoms in 500 to be achieved with this source, but only at the expense of deposition rate. In the samples used in these first experiments, the filtration step was omitted but the method still gives a tighter size distribution than can be obtained by precipitation. The cluster beam was directed onto a substrate simultaneously with a flux of evaporated silver, producing a film of randomly spaced clusters embedded in a non-magnetic matrix. A 20 nm buffer layer of silver was first deposited onto the substrate, followed by the 500 nm cluster-containing layer, capped with 5 nm of silver to protect against oxidation. An effective iron concentration of 0.1% by volume was chosen to minimize dipole–dipole interactions between the clusters. In such a dilute sample, most of the implanted muons stop in the matrix material between the clusters. This contrasts with Mössbauer measurements, where the probe nucleus would lie within a cluster

## 2. Low energy $\mu$SR measurements

The sample for the low energy $\mu$SR measurements was made up from a mosaic of nine, 1 cm$^2$ films on polished silver substrates. The mosaic of films was bonded to a silver plate which was bolted onto the cold finger of the cryostat. The geometry of the low energy $\mu$SR spectrometer is indicated in figure 1. There are four positron detectors around the sample, in the $\pm z$ and $\pm y$ directions. Only the $\pm z$ detectors are shown in figure 1. The initial spin polarization of the incoming muons is along the positive $z$ axis. The field is applied with a Helmholtz pair along the positive $x$ axis, parallel to the incoming beam, and perpendicular to both the muon spin and to the plane of the sample.

Muons with kinetic energy 16 keV were focused by electrostatic lenses to a spot 3 cm in diameter and centred on the sample. Simulations of the stopping of 16 keV muons in silver using the TRIM-SP code [21] showed a mean implantation depth of order 60 nm. The implantation profile is shown in figure 2. The sample was field cooled from room temperature in a field of 25 mT and muon decay spectra were collected at various sample temperatures down to 4.7 K. The count rate of positrons emitted by muons decaying in the sample was of the order of 20 s$^{-1}$.

The timescale of a $\mu$SR measurement is set by the time over which the muon precession and decay are observed, and is of the order 10 $\mu$s. At low temperatures, the moments of the iron clusters are static on this timescale. The static distribution of the local fields within the sample causes the implanted muons to precess out of step, and leads to a damping of the decay

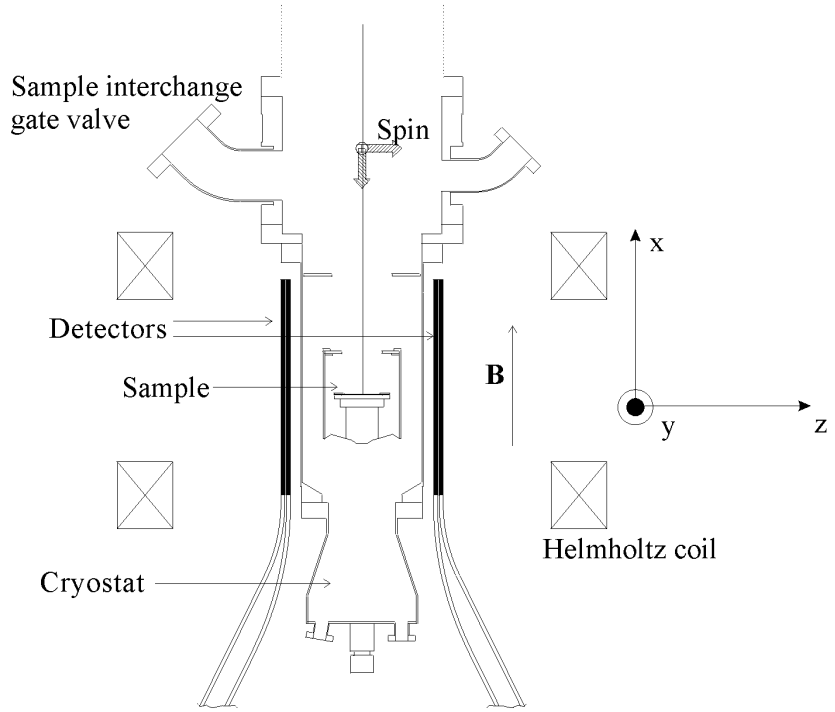


**Figure 1.** Schematic diagram of the low energy $\mu$SR experiment. The magnetic field is applied to the sample along the $x$ direction by a Helmholtz pair. The sample lies in the $yz$ plane. The incident muons are spin polarized along the $z$ direction.

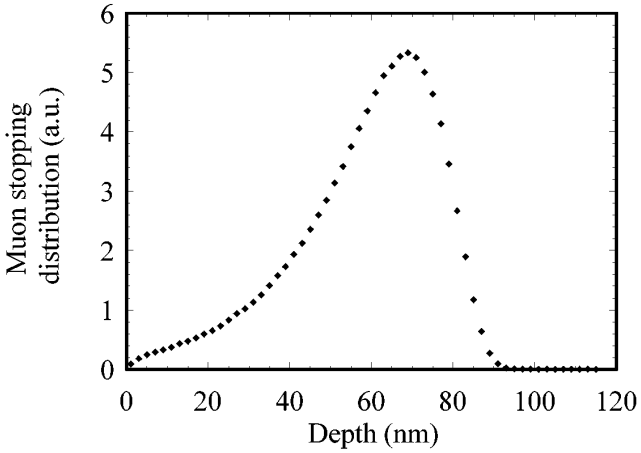


**Figure 2.** Stopping distribution of 16 keV muons in silver. The profile was calculated with the TRIM-SP code [21] modified to include a 0.5 keV Gaussian energy width introduced by the muon detectors in the low energy muon apparatus [18, 19].

positron time spectrum. In the dilute limit, the field distribution due to the static dipole fields of the clusters is Lorentzian, leading to an exponential damping [7, 22].

The decay positron time spectra were fitted in the time domain with a signal of the form

$$[1 + G_{TF}(t)] \exp(-t/\tau_\mu) = [1 + A_i \exp(-(\sigma t)^\beta) \cos(\omega_\mu t + \phi_i)] \exp(-t/\tau_\mu). \quad (5)$$

The cosine term in equation (5) describes the precession of the implanted muons with lifetime $\tau_\mu$ at an angular frequency $\omega_\mu$ defined by the average local field. $\phi_i$ is the phase factor for detector $i$; $A_i$ represents the amplitude of the original muon decay asymmetry [15, 16]. A fixed background signal was included in the fits with an asymmetry of 0.035. This background arose from muons which missed the sample and became implanted in the silver plate. The parameters $\sigma$ and $\beta$ are the muon polarization relaxation rate and relaxation exponent respectively. Theoretical treatments [16, 22] provide justification for fixing the value of the relaxation exponent $\beta$.

For a static Lorentzian field distribution the appropriate value for the relaxation exponent is $\beta = 1$, corresponding to pure exponential damping. In this regime the muon relaxation rate, $\sigma_{Lorentz}$, is related to the half width at half maximum (HWHM) $\Delta B$ of the field distribution by [16, 22]

$$\Delta B = \sigma_{Lorentz}/\gamma_\mu. \quad (6)$$

At higher temperatures, the implanted muons experience rapidly fluctuating random fields, characterized by a relaxation time $\tau$. The correct form of equation (5) in this regime is a 'stretched' exponential with the relaxation exponent $\beta = 0.5$ [16, 22]. The stretched form is a consequence of averaging over different fluctuating local fields at different muon sites. In this regime the muon relaxation rate $\sigma(T)$ is related to the cluster relaxation time $\tau(T)$ by

$$\sigma(T) = 4(\gamma_\mu \Delta B)^2 \tau(T). \quad (7)$$

At first sight it may appear that both relaxation parameters, $\sigma$ and $\beta$ can be treated as free parameters in fits of the decay positron time spectra to equation (5). Such an approach may produce spurious results, however good the statistics of the data, because $\sigma$ and $\beta$ are highly correlated. In this work we have followed the theoretical indications outlined above and *fixed* the value of the relaxation exponent $\beta$ to that appropriate for the temperature range: $\beta = 1$ in the range 4.7 K to 15 K, and $\beta = 0.5$ in the range 20 K to 300 K.

Examples of fits of decay positron time spectra from the detector in the positive $z$ direction in figure 1, are shown in figures 3(a) and 3(b). The time independent backgrounds and the exponential decay due to the muon lifetime have been removed in order to show the time evolution of the muon asymmetry. The solid lines are the results of fits to equation (5). Figure 3(a) shows data from the measurement at 4.7 K. In this case, the relaxation exponent $\beta$ was fixed with a value of unity. The data clearly show an exponential relaxation. The increase in the size of the error bars at long times results from the muon lifetime (2.2 $\mu$s). The total data from each run was four such spectra, one from each detector. Figure 3(b) shows data from the measurement at 300 K. In this case, the relaxation exponent $\beta$ was fixed with a value of 0.5. The relaxation is much slower: thermal activation of the cluster moments produces an effective narrowing of the field distribution experienced by the implanted muons.

The muon relaxation rate $\sigma$ deduced from fits to equation (5) of all the data is shown as a function of temperature in figure 4(a). The open symbols show the results of fits to the data at temperatures up to and including 15 K, fits in which the value of $\beta$ was fixed to unity. The dark symbols show the results of fits to the data at 20 K and above, fits in which the value of $\beta$ was fixed to 0.5. The choice of these temperature intervals is seen to be consistent with the data as viewed in figures 3 and 4(a). It is verified by the blocking temperature measured by SQUID magnetometry and by simulations of the low temperature field distribution (sections 3 and 4 below). The fitting procedure was tested directly with artificial data constructed with similar statistics and relaxation parameters.

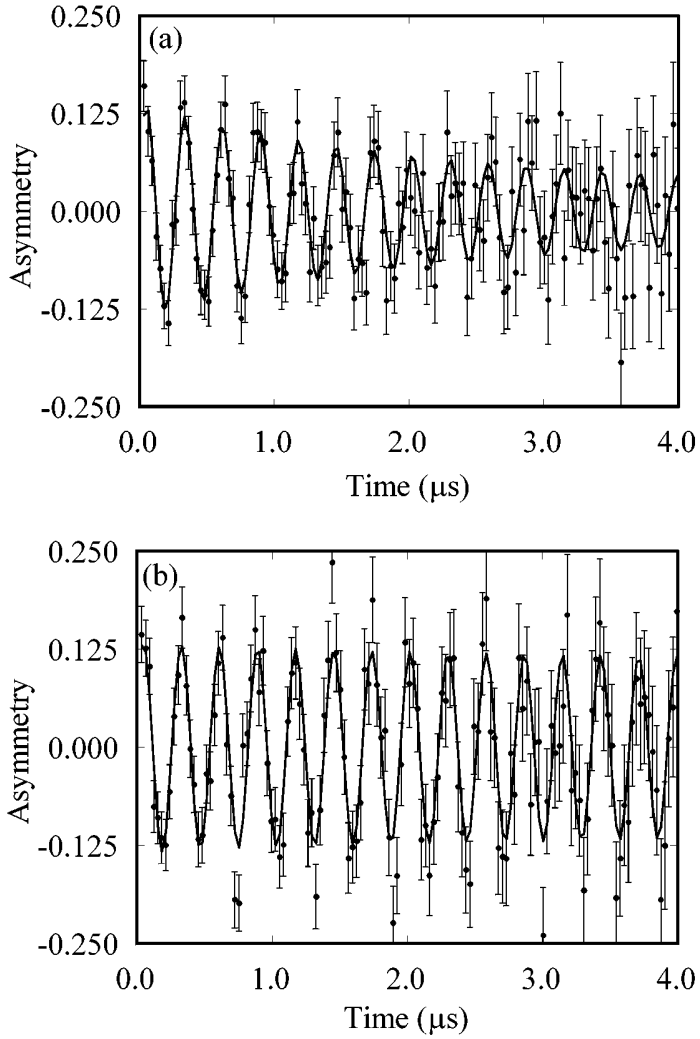


**Figure 3.** Asymmetry plots, $G_{TF}(t)$ in equation (5), from the detector in the positive $z$ direction with the sample at (a) 4.7 K and (b) 300 K. The data have been packed into bins of width 30 ns for publication purposes. In both figures, the solid lines are fits to equation (5), with fixed relaxation exponent $\beta = 1$ at 4.7 K and fixed relaxation exponent $\beta = 0.5$ at 300 K.

The low temperature data show an average damping rate of $\sigma_{Lorentz} \approx 0.4\ \mu$s. This relaxation rate corresponds to a static Lorentzian distribution of local fields with an HWHM $\Delta B \approx 0.5$ mT.

The high temperature data in the range 20–300 K are re-plotted on an Arrhenius plot in figure 4(b). The damping rate arising from a thermally activated process involving a single activation energy $E_A$ should obey an Arrhenius law,

$$\sigma(T) = \sigma_0 \exp(E_A/k_BT) \tag{8}$$

which may be re-arranged to give the standard Arrhenius plot

$$\log_e \sigma = \log_e \sigma_0 + E_A/k_BT. \tag{9}$$

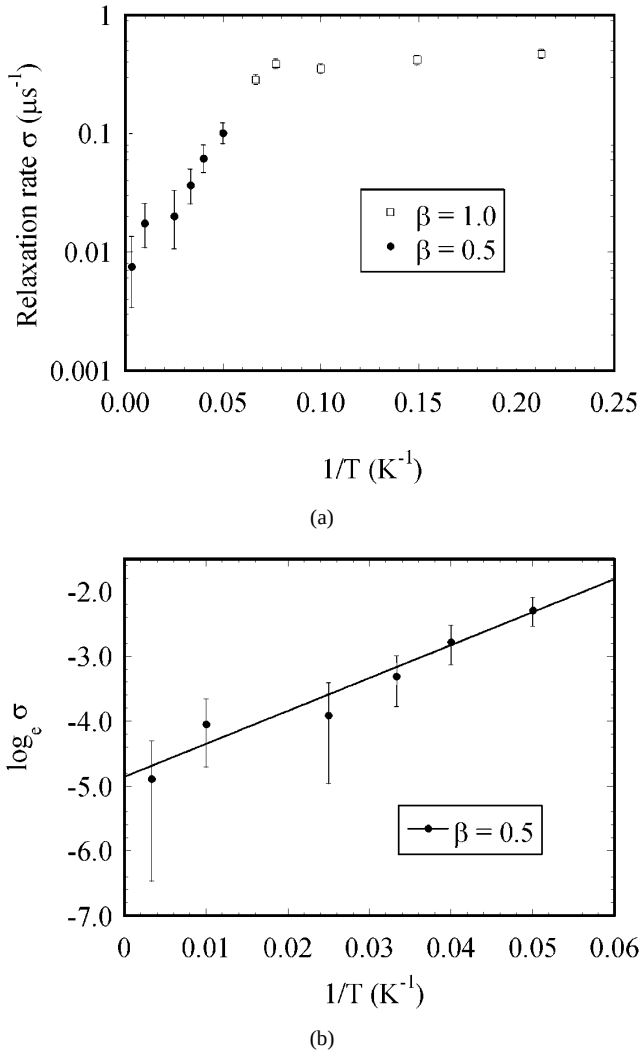


**Figure 4.** (a) The muon relaxation rate $\sigma$ from fits to equation (5). The open symbols show the results of fits of the data from 4.7 K to 15 K with the fixed relaxation exponent $\beta = 1$. The dark symbols show the results of fits of the data from 20 K to 300 K with the fixed relaxation exponent $\beta = 0.5$. (b) Arrhenius plot of the muon relaxation rate at high temperatures (20–300 K). The slope gives an energy barrier of $51 \pm 9$ K. The $y$-intercept corresponds to a muon relaxation rate of $\sigma_0 = 8 \pm 3$ ns$^{-1}$, equivalent to an intrinsic cluster relaxation time of $\tau_0 = 12 \pm 4$ ns.

The intercept in figure 4(b) gives an intrinsic damping rate of $\sigma_0 = 8 \pm 3$ ns$^{-1}$. Using equations (1) and (7), we deduce an intrinsic cluster relaxation time of $\tau_0 = 12 \pm 4$ ns. The linear slope of the data in figure 4(b) gives an activation energy of $E_A = 51 \pm 9$ K. If we assume that the cluster volume is $1.2 \times 10^{-26}$ m$^3$, as suggested by the magnetometry data presented below, we find a cubic anisotropy constant of $K = 2.3 \pm 0.4 \times 10^5$ J m$^{-3}$. This enhancement by a factor of five over the bulk value is consistent with the enhanced orbital moment found previously for similar clusters [23]. The enhancement arises from the reduced co-ordination of the atoms at the surface of a cluster, which results in an incomplete quenching of the orbital moment.

### 3. Magnetization measurements

Measurements of the field- and temperature-dependent magnetization were performed in a SQUID magnetometer with a 1.5 $\mu$m thick test sample deposited on a high purity graphite substrate. The large perpendicular susceptibility of graphite precluded measurements with the field applied perpendicular to the sample plane, other than remanence measurements in zero field.

Magnetization loops at several temperatures, plotted against $(B_{app}/T)$, are shown in figure 5, together with a Langevin curve computed using a saturation magnetization of $2 \times 10^{-8}$ A m$^2$ and a cluster moment of 2267 $\mu_B$. This moment corresponds to a volume of $1.2 \times 10^{-26}$ m$^3$, if we assume the bulk density of atoms, $8.49 \times 10^{28}$ m$^{-3}$, and an enhanced moment per atom of 2.3 $\mu_B$ [23]. The magnetization of each cluster is then $\mu_0 M = 2.2$ T. At 5 K the data in figure 5 deviate from superposition, indicating the presence of blocking at this temperature.

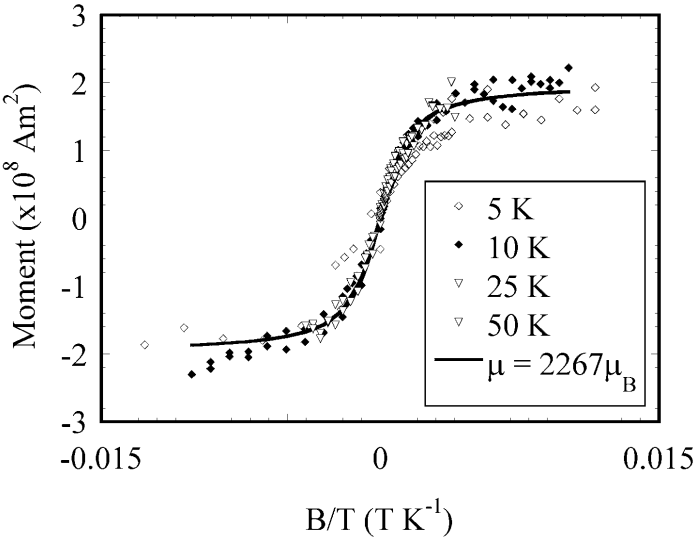


**Figure 5.** Magnetization loops of the cluster samples, plotted against $(B_{app}/T)$ to show the presence of superparamagnetic behaviour above 5 K. The solid line is the prediction of the Langevin function, at 10 K, for clusters of moment 2267 $\mu_B$.

Figure 6 shows the decay of the remanence, for fields applied parallel (full symbols) and perpendicular (open symbols) to the plane of the sample. The data were taken by zero field cooling to 4 K, followed by application of a 0.1 T field. The field was then removed and the remanent moment measured. The application/removal procedure was repeated at each temperature as the sample was warmed. The similarity between the sets of data in figure 6 indicates that the assembly of isolated clusters is not magnetically harder perpendicular to the film plane than parallel to the plane. The absence of a preferred orientation, in or out of the sample plane, is in agreement with x-ray magnetic circular dichroism measurements reported previously [23].

The maximum remanent magnetization of randomly oriented, blocked clusters with cubic magnetocrystalline anisotropy, has been calculated to be 0.832 $M_s$ [24]. We find (in figure 6) that the remanence is already as low as one-fifth of the saturation moment at 5 K, so blocking is not complete at this temperature. However, the remanence disappears completely by 10 K,

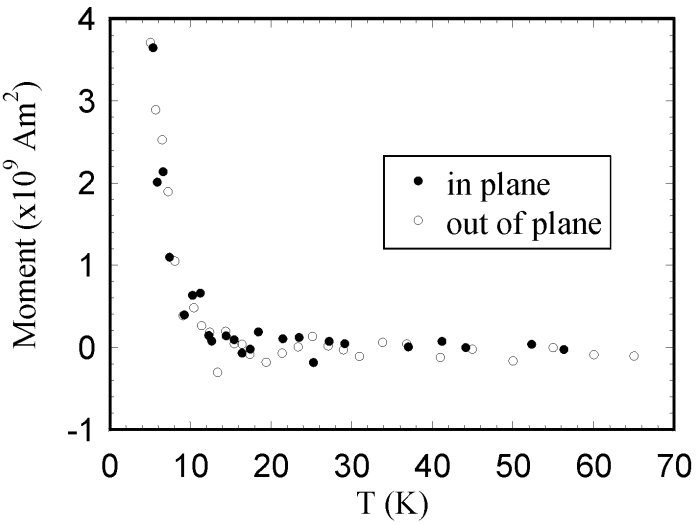


**Figure 6.** In plane (solid symbols) and out of plane (open symbols) remanence data, showing lack of a preferred orientation for the magnetization of the cluster assembly.

which is evidence for a tight size distribution amongst the clusters. We have not attempted to fit a size distribution to these data because we have data only at relatively high temperatures. Furthermore, at present we have no knowledge of the form of the distribution we expect for these embedded clusters. However we note that work elsewhere on *bare* clusters has shown the clusters to follow a log normal size distribution, with median diameter 2.8 nm and width 0.5 nm [20].

The zero field cooled (ZFC) magnetization was measured by zero field cooling the sample from 120 K to 4 K, followed by data acquisition on warming in a field applied parallel to the film plane. Measuring fields of 3 mT, 5 mT, 15 mT and 25 mT were used. The ZFC data are shown in figure 7(a). At very low temperatures, the relaxation time of at least some of the clusters is much longer than the measurement timescale (100 s per point). As the temperature is increased the relaxation time decreases, so the susceptibility rises. At high temperatures, the relaxation time is much smaller than the measurement time so the clusters show superparamagnetic behaviour with a susceptibility which varies as $T^{-1}$. The maximum in the susceptibility occurs at the 'blocking temperature', when the relaxation time and measurement time are equal [25]. The temperature of the maximum in figure 7(a) appears to have increased with increasing field, and to extrapolate to 4 K in zero field. However, the true effect of the field is to flatten the equilibrium $M(T)$ curves, as described by the Langevin function [1]. In figure 7(b), we plot the ZFC data normalized by the Langevin function, at each field. The deviations from the Langevin prediction (which assumes the attainment of an equilibrium magnetization and a negligible anisotropy parameter $\alpha$) are independent of the applied field. This result shows the fields used here to have a rather small effect on the blocking temperature and therefore on the relaxation time. Theoretical work concerning uniaxial anisotropy potentials [14] has shown that the relaxation time is decreased by application of a magnetic field. The influence of the field depends on the ratio $h$ of the applied field to the anisotropy field: $h = M_s B_{app}/2K$. Using the enhanced value of $K$ as determined for our clusters in section 2 above, we find $h \approx 0.09$ when the applied field $B_{app} = 0.025$ T. This small value explains the weak influence of the applied field on the ZFC measurements.

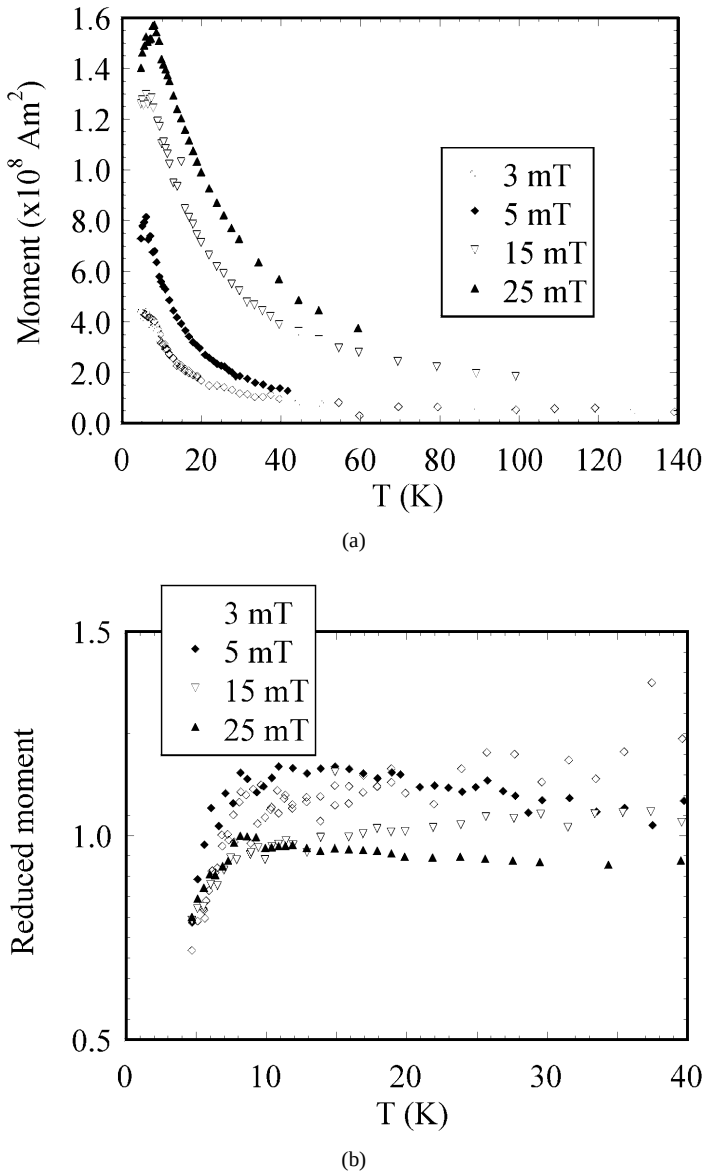


**Figure 7.** (a) Zero field cooled magnetization data measured in 3 mT, 5 mT, 15 mT and 25 mT. (b) ZFC data after division by the Langevin function. The Langevin function describes the unblocked magnetic behaviour of superparamagnetic particles in the low anisotropy limit.

## 4. Simulations of the dipole field

Simulations of the dipole field within a cluster sample are important to understand the $\mu$SR results. In the simulations, we calculated the (low temperature) field distribution given by the muon decay positrons arriving at the $\pm y$ detectors in figure 1, when a magnetic field of 25 mT was applied along the $x$ direction. The net local field at a muon site is the resultant of the dipolar fields, due to a random arrangement of clusters of magnetization $\mu_0 M_s = 2.2$ T at

a concentration 0.1% by volume, and the applied field. Each muon precesses at a rate given by the magnitude of this local field. To produce a simulated spectrum, the amplitude of the precession was weighted by the sine squared of the angle between the local field and the initial direction of the muon spin.

Two illustrative simulations were performed. When the dipoles were ordered along the positive $z$ direction, an FWHM of $1.4 \pm 0.1$ mT was calculated after averaging over five simulations, each run with different random seeds. A second set of simulations, in which random disorder was introduced into the orientation of the dipoles within the $zy$ plane, produced the same field width. The simulations indicate that the orientation of the clusters' moments, when the clusters are static at low temperatures, has a negligible effect on the distribution of dipolar fields within the sample. The simulations gave the expected Lorentzian field distribution, with an HWHM $\Delta B = 0.7$ mT. The corresponding low temperature muon depolarization rate, of approximately $0.6\ \mu s^{-1}$, is consistent with the value of $\sigma_{Lorentz}$ derived from the experimental data.

$\mu$SR studies of magnetic relaxation in spin glasses [22] are often performed in a longitudinal geometry, where the applied field is parallel to the initial muon spin direction. In this case the fluctuating magnetic moments at high temperatures cause a weak damping in the muon decay spectra, due to the inducing of transitions which depolarize the muons. The maximum damping rate is $4\gamma_\mu(\Delta B)^2/B_{app}$, so damping due to this cause is suppressed by the applied field.

In principle, the diffusion of muons within the sample could lead to a motional narrowing effect on top of the effect produced by fluctuations of the clusters' moments. Extrapolation of the published data on muon diffusion in silver shows that below 200 K the muon occupies a single octahedral or tetrahedral site within the silver lattice. At 300 K, where the muon relaxation rate is already small, the diffusion length within the muon lifetime is of the order of 5 nm [15], which should have a small effect. The nuclear moment of silver is known to be too small to make any noticeable contribution to the observed field width.

## 5. Conclusions

The experiments reported here are the first measurements of dynamic magnetic behaviour in thin films to be taken with the new low energy $\mu$SR spectrometer at the Paul Scherrer Institut. We have shown that the method may be used to extract parameters such as the relaxation time and activation energy of an assembly of ferromagnetic clusters displaying superparamagnetic behaviour. In these experiments, on iron clusters in silver, we find an intrinsic relaxation time of $\tau_0 = 12 \pm 4$ ns and an activation energy of $\Delta E = 51 \pm 9$ K for clusters of volume $1.2 \times 10^{-26}$ m$^3$. With the assumption of cubic anisotropy, we find an anisotropy constant of $K = 2.3 \pm 0.4 \times 10^5$ J m$^{-3}$. The anisotropy parameter $\alpha$ in equation (4) then lies in the range $0.2 < \alpha < 3$ between 300 and 20 K respectively. Therefore, at highest measurement temperature, the relaxation time defined in equations (2) and (3) may be calculated by assuming that the value of $\lambda_1$ is close to 2 [11, 13]. The theoretical relaxation time is given by $\tau_D$ in equation (3), where $\tau_D \approx 10^{-11}(1+a^2)/a$. The experimentally derived value for the relaxation time at this temperature, of the order of $10^{-8}$ s, suggests a large value for the damping parameter $a$, and that perhaps these nanoclusters are highly defective [9].

The lack of any preferred orientation in the cluster assembly allows direct comparison of the $\mu$SR and SQUID data, which were taken with the applied field perpendicular and parallel to the sample plane respectively. The two techniques examine the clusters' behaviour over very different timescales. In the SQUID the time taken to settle at the next temperature and take three readings for averaging was of the order of 100 s. There was no change in the data

above the noise during the time taken to make the three readings. The timescale in $\mu$SR is of the order of 10 $\mu$s and is determined by the muon lifetime. Equation (1) then suggests that the blocking temperature for the muon data should be approximately three times that recorded in the SQUID, or approximately 20 K. There is thus an internal consistency in our use of the low energy $\mu$SR data above 20 K to determine the relaxation time and activation energy.

Recent developments of the gas condensation source used to deposit the clusters now allow the deposition of clusters of diameter 2 nm with 5% resolution in time periods appropriate for thin film deposition. Furthermore, the kinetic energy with which these highly selected clusters are deposited onto the substrate may now be controlled with electrostatic acceleration grids. This affords control over deformation of the clusters when they lose their kinetic energy and come to rest on the substrate, and the possibility of control over the shape anisotropy. Since the clusters arrive on the substrate at an angle of 45°, the production of aligned samples may be feasible, from which angular dependencies in the relaxation time may be measured and the dissipation parameter $a$ determined more clearly [4].

## Acknowledgments

We are grateful for financial support from the UK Engineering and Physical Sciences Research Council (grant number GR/K87753), the German BMBF and to the Paul Scherrer Institut for beamline facilities. The TRIM-SP code for prediction of the stopping depths of low energy muons was kindly provided by W Eckstein, Max Planck Institut für Plasmaphysik, Garching, Germany.

## References

[1] Jacobs I S and Bean C P 1963 Fine particles, thin films and exchange anisotropy *Magnetism* vol III, ed G T Rado and H Suhl (New York: Academic) pp 271–350
[2] Bødker F, Mørup S, Pedersen M S, Svedlinh P, Jonsson G T, Garcia-Palacios J L and Lazaro F J 1998 *J. Magn. Magn. Mater.* **177–181** 925
[3] Wernsdorfer W, Bonet Orozco E, Hasselbach K, Benoit A, Barbara B, Demoncy N, Loiseau A, Pascard H and Mailly D 1997 *Phys. Rev. Lett.* **78** 1791
[4] Coffey W T, Crothers D F S, Dormann J L, Kalmykov Yu P, Kennedy E C and Wernsdorfer W 1998 *Phys. Rev. Lett.* **80** 5655
[5] Bellouard C, Mirebeau I and Hennion M 1995 *J. Magn. Magn. Mater.* **140–144** 431
[6] Casalta H, Schleger P, Bellouard C, Hennion M, Mirebeau I, Ehlers G, Farago B, Dormann J-L, Kelsch M, Linde M and Phillip F 1999 *Phys. Rev. Lett.* **82** 1301
[7] Bewley R I and Cywinski R 1998 *Phys. Rev.* B **58** 11 544
[8] Brown W F 1979 *IEEE Trans. Magn.* **15** 1196
[9] Coffey W T, Crothers D F S, Dormann J L, Geogehan L J, Kennedy E C and Wernsdorfer W 1998 *J. Phys.: Condens. Matter* **10** 9093
[10] Eisenstein I and Aharoni A 1977 *Phys. Rev.* B **16** 1278
[11] Kalmykov Yu P, Titov S V and Coffey W T 1998 *Phys. Rev.* B **58** 3267
[12] Kalmykov Yu P and Titov S V 1999 *Phys. Rev. Lett.* **82** 2967
[13] Aharoni A 1973 *Phys. Rev.* B **7** 1103
[14] Coffey W T, Crothers D F S, Dormann J L, Geogehan L J and Kennedy E C 1998 *Phys. Rev.* B **58** 3249
[15] Schenck A 1985 *Muon Spin Rotation Spectroscopy* (Bristol: Hilger)
[16] Uemura Y J 1999 $\mu$SR relaxation functions in magnetic materials *Muon Science* ed S L Lee, S H Kilcoyne and R Cywinski (Bristol: Institute of Physics Publishing) p 85–114
[17] Morenzoni E, Kottmann F, Maden D, Matthias B, Meyberg M, Prokscha Th, Wutzke Th and Zimmermann U 1994 *Phys. Rev. Lett.* **72** 2793
[18] Morenzoni E, Birke M, Glückler H, Hofer A, Litterst J, Meyberg M, Niedermayer Ch, Prokscha Th, Schatz G and Wutzke Th 1997 *Hyperfine Interact.* **106** 229
[19] Glückler H *et al Physica* B at press

[20] Baker S H, Thornton S C, Keen A M, Preston T, Norris C, Edmonds K W and Binns C 1997 *Rev. Sci. Instrum.* **68** 1853
[21] Eckstein W 1991 *Computer Simulation of Ion–Solid Interactions* (Berlin: Springer)
[22] Uemura Y J, Yamazaki T, Harshman D R, Senba M and Ansaldo E J 1985 *Phys. Rev.* B **31** 546
[23] Edmonds K W, Binns C, Baker S H, Thornton S C, Norris C, Goedkoop J, Finazzi M and Brookes N 1999 *Phys. Rev.* B **60** 472
[24] Gans R 1932 *Ann. Phys. Lpz.* **15** 28
[25] Gittleman J I, Abeles B and Bozowski S 1974 *Phys. Rev.* B **9** 3891